

# Investigation of Layered Structure of Fiber Cell Wall in Korean Red Pine by Confocal Reflection Microscopy

Ohkyung Kwon\*

*National Instrumentation Center for Environmental Management, Seoul National University, Seoul 151-921, Korea*

\*Correspondence to:  
Kwon O,  
Tel: +82-2-880-4823  
Fax: +82-2-888-4847  
E-mail: zoom@snu.ac.kr

Received June 9, 2014  
Revised June 27, 2014  
Accepted June 27, 2014

Layered structures of fiber cell wall of Korean red pine (*Pinus densiflora*) were investigated by confocal reflection microscopy (CRM). CRM micrographs revealed detailed structures of the fiber cell wall such as S1, S2, and S3 layers as well as transition layers (S12 and S23 layers), which are present between the S1, S2, and S3 layers. Microfibril angle (MFA) measurement was possible for the S2 and S3 layer in the cell wall. The experimental results suggest that CRM is a versatile microscopic method for investigation of layered structures and MFA measurement in individual sub layer of the tracheid cell wall.

**Key Words:** Confocal reflection microscopy, Confocal laser scanning microscopy, Cell wall structure, Layered structure, Microfibril

## INTRODUCTION

Wood fibers have been used as important natural resources to produce variety of materials such as paper, paperboard, tissue, cardboard and fiberboard. Numerous studies have attempted to obtain details of ultrastructure and chemical composition of the fiber because its ultrastructure ultimately impact product properties.

The cell wall of wood fiber has layered structure, which consists of primary wall and secondary wall with sub layers: S1, S2, and S3 layers (Fig. 1). Especially the orientation of cellulose microfibril (MF) or microfibril angle (MFA) has been under great interest because MFA of the fiber cell wall is a key indicator for material properties of the fiber. MFA in S2 layer is highly correlated with material properties of wood (Abe & Funada, 2005; Donaldson, 2008).

MFA in the fiber cell wall has been investigated by various methods such as X-ray diffraction (XRD) (Cave, 1997), wide-angle X-ray scattering (WAXS) (Entwistle et al., 2007) and small-angle X-ray scattering (SAXS) (Andersson et al., 2000), near infra-red (NIR) (Hein et al., 2010), polarization light microscopy (PLM) (Leney, 1981), differential interference contrast (DIC) microscopy (Peter et al., 2003), confocal laser scanning microscopy (CLSM) (Sedighi-Gilani et al.,

2005), confocal reflection microscopy (CRM) (Donaldson & Frankland, 2004), transmission electron microscopy (TEM) (Donaldson & Xu, 2005) and scanning electron microscopy (SEM) (Brandstrom, 2004; Abe & Funada, 2005). For further details, there are several extensive reviews and studies regarding MFA related subjects (Barnett & Bonham, 2004; Abe & Funada, 2005; Donaldson, 2008).

Among the MFA measurement techniques, TEM has been a microscopic technique clearly displaying MF arrangement in the sub layers of the secondary wall (Reis & Vian, 2004; Donaldson & Xu, 2005), but size of field of view (FOV) is very limited. SEM has advantage in the size of FOV, but it is a method of surface topology, which structures only within a few decades of nanometer deep from the surface can be detectable. Thus, it requires special sample preparation steps to reveal the surface of the sub layers in the secondary wall. Due to these limitations, TEM and SEM were not extensively used for MFA measurement for the fiber cell wall, but for close investigation of MF arrangement in each sub layer of the secondary wall.

On the other hand, light microscopy (LM) allows us to investigate relatively large FOV as well as few-decade micron thick sections from three major planes of wood. Light microscopy such as PLM (Leney, 1981; Andersson et al.,

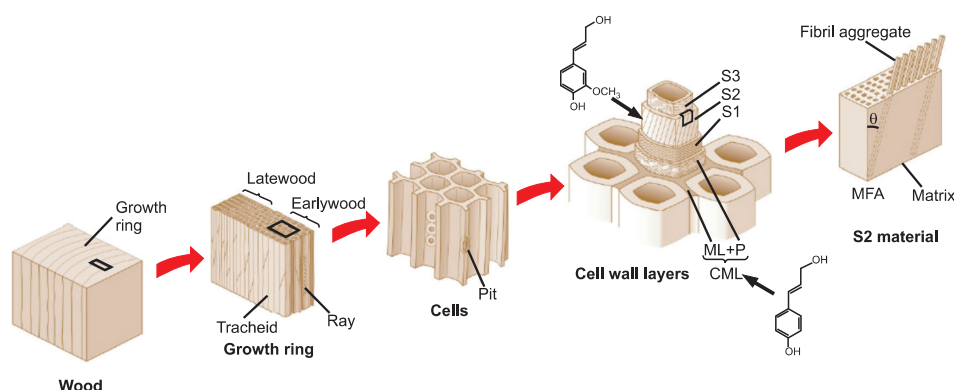


**Fig. 1.** A cell wall model of wood is presented. The cell wall consists of 4 layers (primary, S1, S3, and S3). Middle lamella (ML) is located at between fibers. Monomeric alcohol for lignin in the cell wall and ML is different. Anatomy of wood presented along the different scales (from Institute for Building Materials, ETH Zurich; <http://www.ifb.ethz.ch/research/sinergia>).

2000), DIC microscopy (Anagnost et al., 2002; Peter et al., 2003) and CLSM (Bergander et al., 2002; Palviainen et al., 2004; Sedighi-Gilani et al., 2005) has been used to measure MFA in S2 layer. To obtain appropriate contrast of MF image against background, special sample preparation methods were also applied to the wood fiber specimen prior to image acquisition (Anagnost et al., 2002; Donaldson & Frankland, 2004). CLSM requires fluorescence from specimen, but no fluorescent dyes are necessary for the wood fiber because it naturally fluoresces. PLM and polarization CLSM utilize the fact that intensity of polarized light from the cell wall is related to the MF orientation. However, it was not possible to directly visualize the MF orientation of the sub layers in the secondary cell wall. Recently, transmitted light microscopy was applied to MFA measurement from unstained radial sections of Korean red pine (Kwon et al., 2013). Parameters of optical components such as condenser aperture and color filter were optimized to obtain best contrast from the unstained sections of the red pine. Subsequent experiments for the same sections are possible if necessary.

Although various techniques have used for investigation on ultrastructural details of the cell wall, direct visualization of MFA distribution in the sub layers (S1, S2, and S3 layers) of the secondary wall has not been fully realized. To obtain MFA distributions in the sub layers, non-destructive 3D imaging technique such as CRM is necessary. CRM collects reflected light from specimen, but eliminates light from out-of-focus planes by utilizing a pinhole in front of light detector (Semler et al., 1997; Paddock, 2002). CRM detects reflected light from borders between structures with different refractive indices. Visualization of MF distribution in the fiber cell wall is possible by creation of micro-cavity by iodine precipitation following treatment with nitric acid (Donaldson & Frankland, 2004). The micro-cavity creates greater difference in refractive index between substances of the cell wall and the cavity. If there are natural cavities in the cell wall, the cavities were clearly showed by CRM. From CRM micrographs, the natural cavities were found in severe compression wood fibers. The ultrastructure of the fiber cell wall can be visualized

without any treatment by CRM because the sub layers of the fiber cell wall have different chemical compositions and alignment of cellulose fibrils (Fig. 1). In wood, middle lamella (ML) is mostly comprised of lignin and pectin, but the secondary wall contains cellulose, hemicellulose and lignin. Chemical compositions of S1, S2, and S3 layers and refractive indices of the chemical components such as cellulose and lignin differ from each other (Fengel & Wegener, 1983; Donaldson, 1985; Bergander & Salmen, 2002; Kasarova et al., 2007). Thus, optical properties such as absorption, reflectance, refraction, polarization and fluorescence from each sub layer of the fiber cell wall are expected to be different.

The main purpose of this study is to demonstrate direct visualization of layered structures and MF arrangement in S layers from the fiber cell wall without apparent cavities. CRM micrographs were taken at consecutive focal positions through the fiber cell wall, and then 3D reconstruction software created 3-dimensional images of the fiber cell wall for further investigation on the layered structures and MF distributions in the fiber cell wall.

## MATERIALS AND METHODS

Radial sections (20  $\mu\text{m}$  thick) of small blocks of red pine (*Pinus densiflora*) were prepared by utilizing a sliding microtome (HM 430; Thermo Scientific Microm, Germany). The unstained sections were mounted on a slide glass with cover slip using double-distilled water as mounting medium. Macerated fibers were prepared for field emission scanning electron microscope (FESEM) by Franklin method (Franklin, 1945).

FESEM (Supra 55 VP; Carl Zeiss, Germany) was used to obtain MF images on the surface of the macerated fibers. Low kV (2 kV and 640 V) acceleration voltage was applied to obtain more surface details from the macerated fiber.

To implement CRM for thin sections of the red pine sample, Leica TCS SP8 STED (Leica Microsystems, Germany) with 40 $\times$ /1.1 water immersion lens and argon gas laser as excitation light source was used in reflection mode by Acousto-Optical

Beam Splitter (AOBS). With the AOBS in reflection mode, detection range of photomultiplier tube (PMT) was set to include the excitation light (488 nm). The size of the pin hole was set to 1 Airy unit for 488 nm, which results 1.07  $\mu\text{m}$  thick optical section.

Both fluorescence (CLSM) and reflection (CRM) images were collected simultaneously. CLSM image contains signals from fluorescent components in the cell wall of the fiber, which is primarily lignin. The fluorescent signal is proportional to concentration of the fluorescent components. On the other hand, CRM detects reflected light from the interface between the layers in the cell wall. The reflection between the layers is caused by different optical properties caused by different chemical compositions (Fengel & Wegener, 1983; Bergander & Salmen, 2002), refractive indices of the chemical constituents (Donaldson, 1985; Kasarova et al., 2007), and the structural organization of the constituents (Fengel & Wegener, 1983; Abe et al., 1997; Bergander & Salmen, 2002; Brandstrom et al., 2003) of the cell wall. The difference in the optical properties enables CRM to create images of the sub layers in the secondary wall.

To generate 3-dimensional image, a stack of images was acquired from consecutive focal positions through the thickness direction in the fiber cell wall. The gap between focal planes were set to at least less than 1/2 of the Z resolution of the objective lens that is determined by numerical aperture (NA) and detecting emission wavelength. In SP8 STED system, thickness of optical section is automatically calculated based on the selected objective lens (40 $\times$ /1.1) and user selected emission wavelength (488 nm; the emission wavelength is the same as the excitation in CRM). Three-dimensional reconstruction for the stack of images was performed to create a volumetric image for investigation of layered structures of the cell wall from various points of view.

## RESULTS

### Structure of the Cell Wall in Cross Section

The secondary wall of wood fiber has known to have sub layers such as S1, S2, and S3 layers. ML adheres wood fibers (Fig. 1). A CRM micrograph showed very distinct separation between ML, S1, S2 and S3 layers (Fig. 2) although ML region was not smooth as expected. From the CRM micrograph (Fig. 2A), layered structures and micro cracks in the cell wall were conspicuous. Regions considered as transition layers (S12 and S23) between the S layers were also visible, which have different chemical and structural compositions from S1, S2 and S3 layers. S12 and S23 layers were considered to have significant variance of MFA from the neighboring S layers. Reflection from the transition layer might be limited by more absorption of the excitation light as well as less reflecting surface structures due to the changes in the structural arrangement of the chemical components such as cellulose, hemicellulose and lignin.

However, layer distinction in a CLSM image was different from the CRM image. For the same region the CLSM micrograph showed distinct difference between ML and the secondary wall (Fig. 2B). The surface facing lumen of the fiber was also brighter than the middle part of the cell wall. This surface was thought to be S3 layer of the secondary wall. No distinction between transition layers was observed from the CLSM image.

The difference was thought to be characteristics of reflected and emitted light from the same object, which reflection is sensitive to alignment of MFs but emitted light comes from deeper part of the layer adding more number of photons detectable.

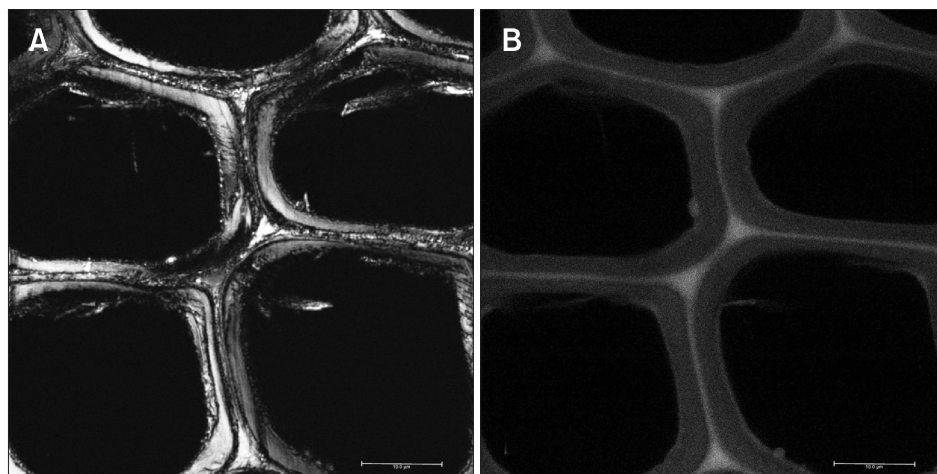


**Fig. 2.** Micrographs by reflection and fluorescence of cross section of Korean red pine by confocal reflection microscopy (A) and confocal laser scanning microscopy (B). Scale bar=10  $\mu\text{m}$ .



### Structure of the Cell Wall in Radial Section

While the sub layers of the cell wall was clearly visible in the CRM micrographs from the cross section of the fiber, complicated distributions of MF orientation was observed from the radial wall (Fig. 3). In the MIP and volume rendered images, various orientation of MF through the cell wall was observed on the radial cell wall and bordered pits. From the images of bordered pits, concentric arrangement of MFs in the border thickening (Fig. 3B, upper two arrows) and net-like arrangement of MFs in margo (Fig. 3B, the diagonal arrow) were visible.

From the reconstructed image, volumetric image (Fig. 4B) as well as cross (Fig. 4D), radial (Fig. 4C) and tangential (Fig. 4A) sectional views of the cell wall were created. The color legend (Fig. 4B) represents depth of the structure from the top. The

lowest parts are in blue, but the highest parts are in red. The closer to the view is in red. Fig. 4A and D showed tangential and cross sectional view of the radial cell wall, respectively. Fig. 4C showed the radial surface corresponding to the depth (=focal position) through cell wall thickness.

Several layers of the secondary wall were observed, but at different positions in the cell wall MF arrangements were appeared to be different (Fig. 4C). Top part of Fig. 4C showed that MF orientation was parallel and perpendicular to the fiber axis, but lower part of the figure displayed those in diagonal to parallel to the fiber axis. This situation was more understandable when MF orientation in Fig. 4C was related to vertical positions in Fig. 4D. Fig. 4C was showing MF arrangements along the blue line in Fig. 4D. The MF arrangement in the top part of the cell wall in Fig. 4C is from

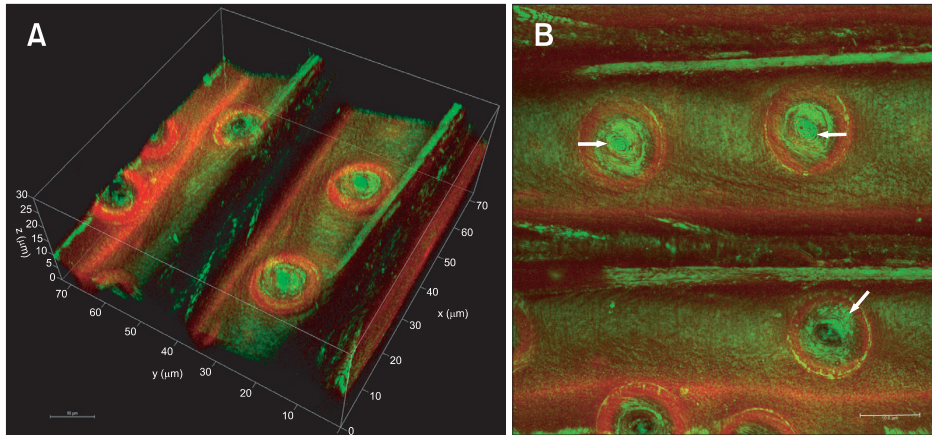


**Fig. 3.** A volume rendered image from Z stacks of confocal reflection micrographs of a radial section of Korean red pine. Various distribution of microfibril angle was observed in the various parts of the radial section. Scale bar=25  $\mu\text{m}$ .

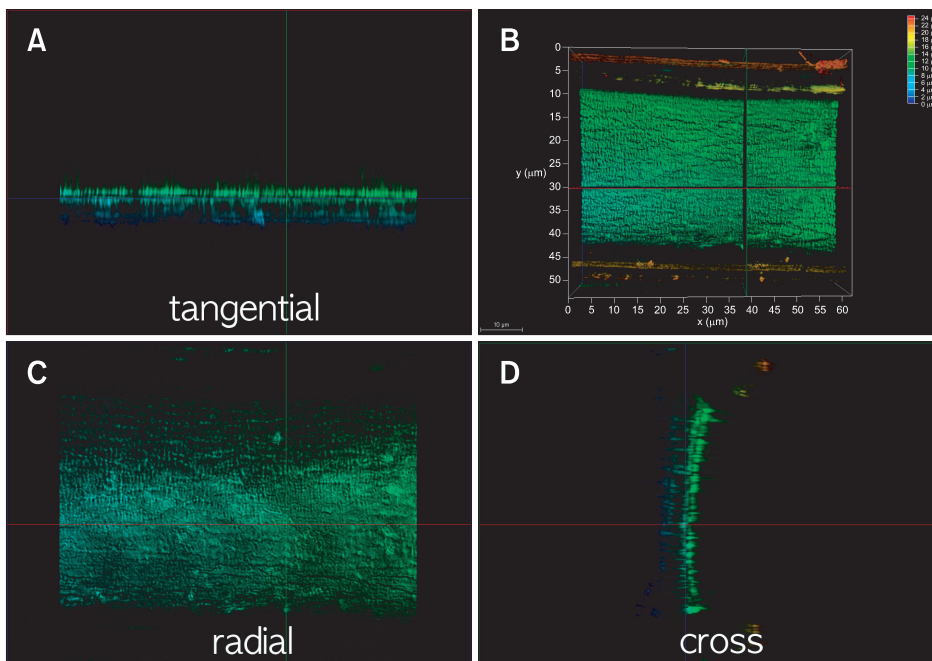


**Fig. 4.** Sectional views of a volume rendered image from Z stacks of confocal reflection micrographs. Tangential (A) and cross (D) sectional views showed several sub layers of the fiber cell wall. The radial surface (C) positioned at the blue line in (A) and (D) showed microfibril orientation at the focal position.

the middle part of S2 layer in Fig. 4D. The middle part of the cell wall showing diagonal arrangement of MF was from the boundary between S2 and S3 layers or S23 layer. This mixture MF orientation of the cell wall seemed to be matched to results from the previous studies regarding MF arrangement in the sub layers of the secondary wall.

Seven layers were observed in the secondary wall (Figs. 4-6). However, actual number of layers might be five, not seven. The top layer in Fig. 5 was thought to be S3 layer and the dark band underneath S3 layer seemed to be a transition layer (S23). The layer at the lowest position in Fig. 5 was thought to be S1 layer, but the dark band directly above S1 layer was considered to be as another transition layer (S12). The layers between S12 and S23 layers were thought to be S2 layer. The center part of S2 layer is dark because S2 layer was thick with compact and uniform arrangement of chemical components, and thus minimal RI differences in S2 layer, especially at the center part. At the interfaces facing towards S12 and S23 layers, certain degree of refractive index mismatch was expected. The amount of reflected light is bigger from the interfaces than from the center of S2 layer. As a result, the seven layers in the figure can be reduced to a layered structure with 5 layers: S3, S23, S2, S12, S1 (from the top of Fig. 5).

MF orientations in S2 and S3 layers were observed from the radial section of the fiber (Fig. 6). When focal position was at S23 layer (Fig. 6A), MFA in the radial surface (Fig. 6B) was perpendicular to the fiber axis. This is consistent to the result from previous studies on MFA of the cell wall although there have not been many experimental results by direct MFA measurement for S3 layer. When focal position was in S2 layer

(Fig. 6A'), MFA in the radial surface (Fig. 6B') was inclined about 35 degrees from the fiber axis. It was considered to be reasonable value as MFA in S2 layer because MFA in S2 layer varies (10~40 degree) depending on growth conditions of tree as well as the part of the cell wall was located between two bordered pits.

Similar MF orientations were observed in FESEM micrographs (Fig. 7). Fig. 7A-C were taken from surface of macerated fiber by Franklin method. It was not easy to determine MF orientation from the FESEM micrographs, but there seemed

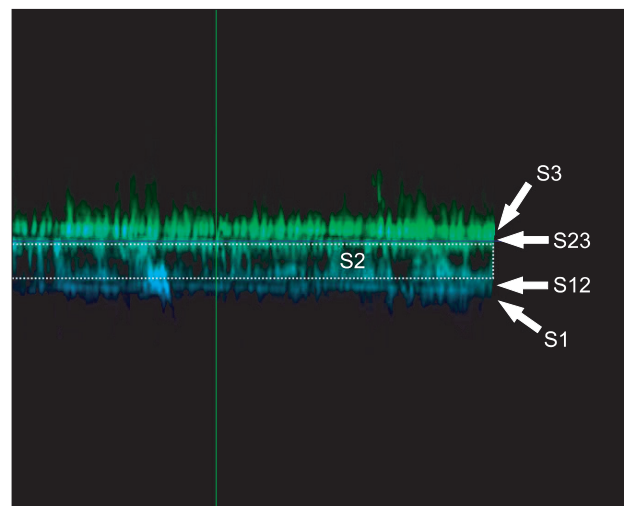


**Fig. 5.** Layered structure of the cell wall in the reconstructed volume image from the Z stack images from at different focal positions through the thickness direction of the cell wall.

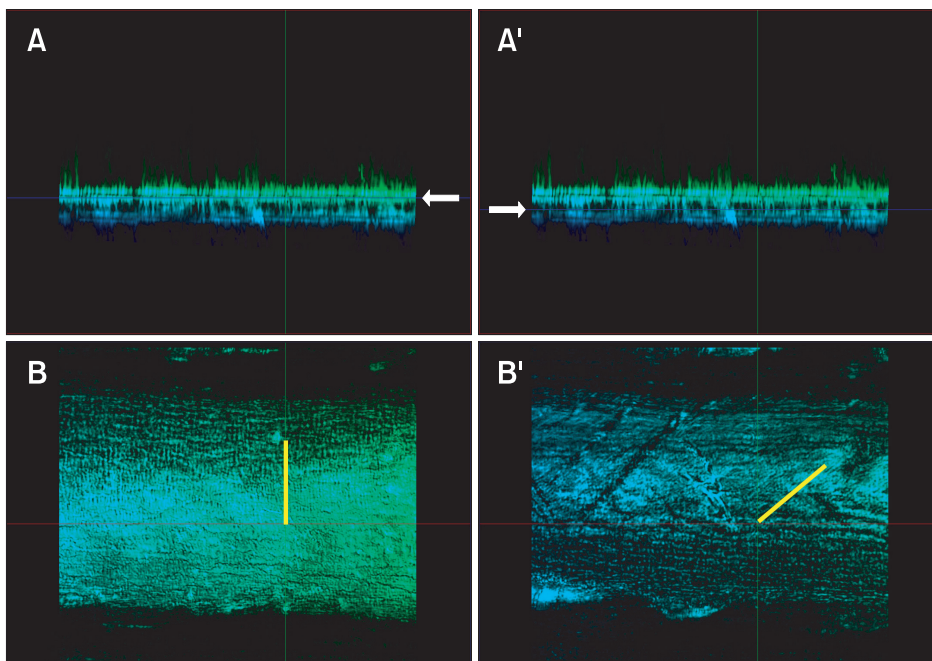


**Fig. 6.** Microfibril orientation according to the positions in the secondary cell wall (arrows). Microfibril orientation almost perpendicular to the fiber axis (B), but diagonal to the fiber axis in a different layer (B') (yellow line).



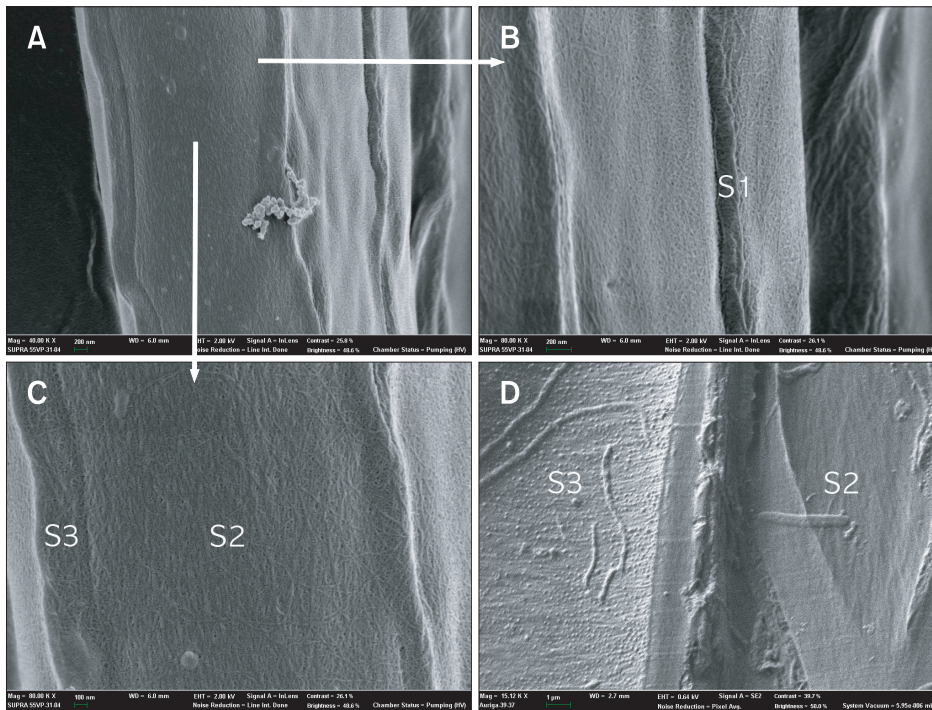


**Fig. 7.** Field emission scanning electron microscope micrographs of fiber cell wall. Macerated fiber prepared by Franklin method (A-C). S1 layer was exposed (B). Microfibril (MF) orientations in S2 and S3 layers were observed differently (C). The similar MF orientation was observed from the view from lumen of the fiber (D). S3 layer showed MF orientation perpendicular to the fiber axis (left side), but S2 layer showed MF orientation off from the fiber axis.

to be different regions with different dominant orientation of MFs. Those regions were considered to be S1, S2 and S3 layers (the labels in Fig. 7B and C). However, no transition layers were clearly definable. MF arrangement of S2 and S3 layers in the radial surface were visible in Fig. 7D. MFA in S3 layer showed perpendicular to the fiber axis, but MFA in S2 layer was inclined from the fiber axis. These observations from the FESEM micrographs were matched to that from the CRM micrographs and reconstructed images.

## DISCUSSION

The difference between CRM and CLSM micrographs can be explained by reflection and emission process of light. Since reflection of light occurs when the waves encounter a surface or other boundary that does not absorb the energy of the radiation and bounces the waves away from the surface, reflected light is more sensitive to orientation and structure of the surface and boundaries in the cell wall. Especially when the surface is very smooth, specular reflection causes very high intensity depending on the direction of detection. No reflection might occur due to material of the layer absorbs most of the incoming light.

On the other hand, properties of emitted light are varied by different chemical compositions in the ML and the secondary wall. The ML is comprised of mostly pectin and lignin from coumaryl alcohol, but the lignin of the secondary wall of softwood such as red pine is coniferyl alcohol (Fig. 1) (Fengel & Wegener, 1983). By 488 nm excitation light, compound

middle lamella (CML) emits more photon than the secondary wall, especially S2 layer. Higher number of photons from CML might be caused by higher concentration of lignin in CML than other layers as well as different chemical composition of ML that is composed of lignin from coumaryl alcohol (Fengel & Wegener, 1983). More emission also comes from S3 layer than S2 layer, but it was not clear why S3 layer emits more photon than S2 layer.

The characteristics of reflected and emitted light can be used as analytical base to investigate chemical and structural compositions of the transition layers. The chemical compositions of S1 layer were thought to be similar to S2 layer because there was no distinctive border between S1 and S2 layer in the CLSM micrograph. However, in the CRM micrograph dark bands between S1 and S2 layers in the cell wall presented regions of the cell wall without reflection. No reflection occurs when incoming light is absorbed by the material of the dark bands, which means that the chemical or structural compositions of the dark regions are very different from the brighter parts (S1 and S2 layer) of the cell wall (Kwon, 2014).

It was shown that MFA of individual S layer is measurable, but more concrete validation of MF distribution in the cell wall is necessary. Validation might be possible only by correlative approaches such as correlative LM and X-ray (CLX) measurement and correlative light and electron microscopy (CLEM). CLEM correlates spatial positions of a CRM micrograph (similar to Fig. 6) to low kV SEM micrographs (similar to Fig. 7) that reveals surface details of uncovered part of the cell wall.

## CONCLUSIONS

Direct visualization of 3-dimensional structures of the fiber cell wall from Korean red pine was performed by 3D reconstruction of stacks of CRM micrographs acquired at different focal positions. The volumetric image from the CRM micrographs clearly revealed the borders between ML, S1, S12, S2, S23 and S3 layers in the fiber cell wall. MFA measurement for each S2 and S3 layer was possible and MFAs in S2 and S3 layers were about 35 and 90 degrees, respectively. The results were reasonably close to the results from previous studies regarding MFA measurement for softwood fiber. Complicated MF orientation around bordered pits was also visible.

Therefore, it was concluded that CRM provides new opportunity to visualize 3-dimensional structures of fiber cell wall and measure MFA in individual sub layer of the secondary wall. Utilizing the MFA from S2 and S3 layers, deeper understanding on physical and mechanical properties related to ultrastructure and MFA in the fiber cell wall is expected.

## CONFLICT OF INTEREST

No potential conflict of interest relevant to this article was reported.

## REFERENCES

- Abe H and Funada R (2005) Review - The orientation of cellulose microfibrils in the cell walls of tracheids in conifers. *IAWA J.* **26**, 161-174.
- Abe H, Funada R, Ohtani J, and Fukazawa K (1997) Changes in the arrangement of cellulose microfibrils associated with the cessation of cell expansion in tracheids. *Trees* **11**, 328-332.
- Anagnost S E, Mark R E, and Hanna R B (2002) Variation of microfibril angle within individual tracheids. *Wood Fiber Sci.* **34**, 337-349.
- Andersson S, Serimaa R, Torkkeli M, Paakkari T, Saranpaa P, and Pesonen E (2000) Microfibril angle of Norway spruce [*Picea abies* (L.) Karst.] compression wood: comparison of measuring techniques. *J. Wood Sci.* **46**, 343-349.
- Barnett J R and Bonham V A (2004) Cellulose microfibril angle in the cell wall of wood fibres. *Biol. Rev.* **79**, 461-472.
- Bergander A, Brandstrom J, Daniel G, and Salmen L (2002) Fibril angle variability in earlywood of Norway spruce using soft rot cavities and polarization confocal microscopy. *J. Wood Sci.* **48**, 255-263.
- Bergander A and Salmen L (2002) Cell wall properties and their effects on the mechanical properties of fibers. *J. Mater. Sci.* **37**, 151-156.
- Brandstrom J (2004) Microfibril angle of the S-1 cell wall layer of Norway spruce compression wood tracheids. *IAWA J.* **25**, 415-423.
- Brandstrom J, Bardage S L, Daniel G, and Nilsson T (2003) The structural organisation of the S-1 cell wall layer of Norway spruce tracheids. *IAWA J.* **24**, 27-40.
- Cave I D (1997) Theory of X-ray measurement of microfibril angle in wood. The condition for reflection X-ray diffraction by materials with fibre type symmetry. *Wood Sci. Technol.* **31**, 143-152.
- Donaldson L (2008) Microfibril angle: measurement, variation and relationships - a Review. *IAWA J.* **29**, 345-386.
- Donaldson L and Frankland A (2004) Ultrastructure of iodine treated wood. *Holzforschung* **58**, 219-225.
- Donaldson L and Xu P (2005) Microfibril orientation across the secondary cell wall of Radiata pine tracheids. *Trees-Struct. Funct.* **19**, 644-653.
- Donaldson L A (1985) Critical assessment of interference microscopy as a technique for measuring lignin distribution in cell walls. *New Zealand J. Forest. Sci.* **15**, 349-360.
- Entwistle K M, Kong K, MacDonald M A, Navaranjan N, and Eichhorn S J (2007) The derivation of the microfibril angle in softwood using wide-angle synchrotron X-ray diffraction on structurally characterised specimens. *J. Mater. Sci.* **42**, 7263-7274.
- Fengel D and Wegener G (1983) *Wood: Chemistry, Ultrastructure, Reactions* (de Gruyter, New York).
- Franklin G L (1945) Preparation of thin section of synthetic resins and wood-resins composite and new mercerization method for wood. *Nature* **155**, 51-55.
- Hein P R G, Clair B, Brancheriau L, and Chaix G (2010) Predicting microfibril angle in Eucalyptus wood from different wood faces and surface qualities using near infrared spectra. *J. near Infrared Spec.* **18**, 455-464.
- Kasarova S N, Sultanova N G, Ivanov C D, and Nikolov I D (2007) Analysis of the dispersion of optical plastic materials. *Opt. Mater.* **29**, 1481-1490.
- Kwon O (2014) Investigation of bordered pit ultrastructure in tracheid of Korean red pine (*Pinus densiflora*) by confocal reflection microscopy. *J. Korean Wood Sci. Technol.* **42**, 346-355.
- Kwon O, Lee M R, and Eom C D (2013) Utilization of light microscopy and FFT for MFA measurement from unstained sections of red pine (*Pinus densiflora*). *J. Korean Wood Sci. Technol.* **41**, 399-405.
- Leney L (1981) A technique for measuring fibril angle using polarized-light. *Wood and Fiber* **13**, 13-16.
- Paddock S (2002) Confocal reflection microscopy: the "other" confocal mode. *Biotechniques* **32**, 274-278.
- Palviainen J, Silvennoinen R, and Rouvinen J (2004) Analysis of microfibril angle of wood fibers using laser microscope polarimetry. *Opt. Eng.* **43**, 186-191.
- Peter G F, Benton D M, and Bennett K (2003) A simple, direct method for measurement of microfibril angle in single fibres using differential interference contrast microscopy. *J. Pulp Pap. Sci.* **29**, 274-280.
- Reis D and Vian B (2004) Helicoidal pattern in secondary cell walls and possible role of xylans in their construction. *Cr. Biol.* **327**, 785-790.
- Sedighi-Gilani M, Sunderland H, and Navi P (2005) Microfibril angle non-uniformities within normal and compression wood tracheids. *Wood Sci. Technol.* **39**, 419-430.
- Semler E J, Tjia J S, and Moghe P V (1997) Analysis of surface microtopography of biodegradable polymer matrices using confocal reflection microscopy. *Biotechnol. prog.* **13**, 630-634.